



Basic Study

Transcriptome sequencing reveals novel biomarkers and immune cell infiltration in esophageal tumorigenesis

Jian-Rong Sun, Dong-Mei Chen, Rong Huang, Rui-Tao Wang, Li-Qun Jia

Specialty type: Oncology

Provenance and peer review:

Unsolicited article; Externally peer reviewed.

Peer-review model: Single blind

Peer-review report's scientific quality classification

Grade A (Excellent): 0

Grade B (Very good): 0

Grade C (Good): 0

Grade D (Fair): D, D

Grade E (Poor): 0

P-Reviewer: Hashimoto N, Japan

Received: November 21, 2023

Peer-review started: November 21, 2023

First decision: December 27, 2023

Revised: January 7, 2024

Accepted: February 4, 2024

Article in press: February 4, 2024

Published online: April 15, 2024



Jian-Rong Sun, Rong Huang, Rui-Tao Wang, School of Clinical Medicine, Beijing University of Chinese Medicine, Beijing 100029, China

Dong-Mei Chen, Li-Qun Jia, Integrated Chinese and Western Medicine Oncology, China-Japan Friendship Hospital, Beijing 100029, China

Corresponding author: Li-Qun Jia, MD, Chief Doctor, Professor, Integrated Chinese and Western Medicine Oncology, China-Japan Friendship Hospital, No. 2 Yinghua East Street, Chaoyang District, Beijing 100029, China. liqun_jia@hotmail.com

Abstract

BACKGROUND

Esophageal squamous cell carcinoma (ESCC) is one of the most common malignancies worldwide, and its development comprises a multistep process from intraepithelial neoplasia (IN) to carcinoma (CA). However, the critical regulators and underlying molecular mechanisms remain largely unknown.

AIM

To explore the genes and infiltrating immune cells in the microenvironment that are associated with the multistage progression of ESCC to facilitate diagnosis and early intervention.

METHODS

A mouse model mimicking the multistage development of ESCC was established by providing water containing 4-nitroquinoline 1-oxide (4NQO) to C57BL/6 mice. Moreover, we established a control group without 4NQO treatment of mice. Then, transcriptome sequencing was performed for esophageal tissues from patients with different pathological statuses, including low-grade IN (LGIN), high-grade IN (HGIN), and CA, and controlled normal tissue (NOR) samples. Differentially expressed genes (DEGs) were identified in the LGIN, HGIN, and CA groups, and the biological functions of the DEGs were analyzed *via* Gene Ontology and Kyoto Encyclopedia of Genes and Genomes enrichment analyses. The CIBERSORT algorithm was used to detect the pattern of immune cell infiltration. Immunohistochemistry (IHC) was also conducted to validate our results. Finally, the Luminex multiplex cytokine analysis was utilized to measure the serum cytokine levels in the mice.

RESULTS

Compared with those in the NOR group, a total of 681541, and 840 DEGs were obtained in the LGIN, HGIN, and CA groups, respectively. Using the intersection of the three sets of DEGs, we identified 86 genes as key genes involved in the development of ESCC. Enrichment analysis revealed that these genes were enriched mainly in the keratinization, epidermal cell differentiation, and interleukin (IL)-17 signaling pathways. CIBERSORT analysis revealed that, compared with those in the NOR group, M0 and M1 macrophages in the 4NQO group showed stronger infiltration, which was validated by IHC. Serum cytokine analysis revealed that, compared with those in the NOR group, IL-1 β and IL-6 were upregulated, while IL-10 was downregulated in the LGIN, HGIN, and CA groups. Moreover, the expression of the representative key genes, such as S100a8 and Krt6b, was verified in external human samples, and the results of immunohistochemical staining were consistent with the findings in mice.

CONCLUSION

We identified a set of key genes represented by S100a8 and Krt6b and investigated their potential biological functions. In addition, we found that macrophage infiltration and abnormal alterations in the levels of inflammation-associated cytokines, such as IL-1 β , IL-6, and IL-10, in the peripheral blood may be closely associated with the development of ESCC.

Key Words: Esophageal squamous cell carcinoma; Intraepithelial neoplasia; Tumorigenesis; Transcriptome sequencing; Biomarkers; Immune cell infiltration; 4-nitroquinoline 1-oxid

©The Author(s) 2024. Published by Baishideng Publishing Group Inc. All rights reserved.

Core Tip: The development of esophageal squamous cell carcinoma (ESCC) involves a stepwise progression from intraepithelial neoplasia to carcinoma. Examining the genes and immune cell infiltration in the microenvironment associated with the multi-stage progression of ESCC is essential for facilitating diagnosis and early intervention. A total of 86 crucial genes linked with ESCC development were discovered using transcriptome sequencing. These genes were enriched in pathways related to keratinization, epidermal cell differentiation, and interleukin (IL)-17 signaling. Additionally, the infiltration of macrophages and abnormal alterations of inflammation-associated cytokines (*e.g.*, IL-1 β , IL-6, and IL-10) in peripheral blood may be strongly linked with the development of ESCC.

Citation: Sun JR, Chen DM, Huang R, Wang RT, Jia LQ. Transcriptome sequencing reveals novel biomarkers and immune cell infiltration in esophageal tumorigenesis. *World J Gastrointest Oncol* 2024; 16(4): 1500-1513

URL: <https://www.wjgnet.com/1948-5204/full/v16/i4/1500.htm>

DOI: <https://dx.doi.org/10.4251/wjgo.v16.i4.1500>

INTRODUCTION

Esophageal cancer (EC) is the seventh most prevalent cancer worldwide. In 2020, there were 604100 new cases and 544000 deaths due to EC[1]. EC can be histopathologically classified into two groups: Squamous cell carcinoma (SCC) and adenocarcinoma (AC). SCC is the most common form of EC and accounts for 80% of all cases globally[2]. SCC originates from low-grade intraepithelial neoplasia (LGIN) and progresses to high-grade IN (HGIN) and carcinoma (CA). Currently, the mechanisms underlying the development and progression of ESCC are largely unknown. Therefore, studying the mechanisms underlying ESCC development and identifying biomarkers are crucial for timely detection, diagnosis, and treatment.

Individual differences may cause heterogeneity in esophageal samples collected during cross-sectional studies, potentially leading to biased results. However, this issue can be addressed by using animal models. The chemical carcinogen 4-nitroquinoline 1-oxide (4NQO) can induce the development of ESCC in mice, similar to the development of ESCC in humans[3,4]. This multistage esophageal carcinogenesis may lead to the discovery of the molecular traits of ESCC through RNA sequencing (RNA-seq) of the transcriptome.

A multistage mouse model of ESCC tumorigenesis was established, and RNA-seq was performed in the present study. Transcriptomic profiling revealed the molecular features of esophageal tumor formation, illustrated the role of these features in determining pathological grade, and revealed a set of key genes associated with the development of ESCC. Furthermore, we studied the pattern of immune cell infiltration in ESCC. These findings illuminate the molecular changes that occur during the development of ESCC in animal models and may have implications for managing human ESCC.

MATERIALS AND METHODS

Materials

4NQO was acquired from Sigma-Aldrich. Antibodies against S100a8, Krt6b, Ki-67, and CD68 were purchased from Cell Signaling Technology. Antibodies against CD80 and CD86 were obtained from Proteintech. Antibodies against CK5 and p40 were purchased from Servicebio.

Induction of esophageal tumorigenesis model

A total of 35 mice were included in this study, 30 of which were assigned to the 4NQO treatment group and 5 to the control group. Animals of eight-week-old C57BL6 mice were purchased from the Beijing Changyang Xishan Breeding Center and were maintained in a local housing facility under a controlled conditions (23 ± 1 °C, $50\% \pm 10\%$ humidity and 12-12 h light-dark cycle). Mice were administered 4NQO (100 µg/mL) in their drinking water for 16 wk to stimulate esophageal carcinogenesis. Freshly-prepared drinking water containing the carcinogen was administered once a week, and the mice had free access to drinking water during treatment. After 16 wk of carcinogen exposure, the mice received sterile water instead of 4NQO-containing drinking water until the end of the 24th wk. In addition, in the control group in which mice were not treated with 4NQO and were fed until the end of the 24th wk.

The animals were euthanized according to the accepted method of euthanasia as defined by the American Veterinary Medical Association Guidelines on Euthanasia-Approved Euthanasia Method, 2013. At the end of the 24th wk, the animals were euthanized with ketamine (100 mg/kg body weight) intraperitoneally as well as *via* a secondary method of cervical dislocation.

Immediately after euthanasia, the esophagus was isolated and rinsed with PBS. The esophagus was frozen at -80 °C for RNA-seq analysis and subsequently fixed in 10% formalin. Paraffin-embedded tissues were sectioned to a thickness of 4 µm for hematoxylin and eosin (HE) staining and immunohistochemistry (IHC).

Two pathologists identified the esophageal lesions based on previously established histopathological criteria[5]. In summary, the normal (NOR) stage consists of a well-oriented, stratified epithelium with a basal zone and a superficial zone. IN is characterized by loss of polarity in epithelial cells, hyperchromatic nuclei with pleomorphism, and increased or abnormal mitotic activity. In LGIN, these abnormalities occur in less than 50% of the epithelium. In high-grade IN (HGIN), however, these changes are present in 50% or more of the epithelium. Lesions that exhibit abnormal changes throughout the entire thickness of the epithelium or invade subepithelial tissues are classified as CA[6].

After clarifying the esophageal pathology *via* HE staining, we randomly selected three samples each of esophageal tissues portraying the LGIN, HGIN, and CA pathological stages in the 4NQO treatment group and three samples of NOR in the control group for subsequent transcriptome sequencing.

RNA-seq

Total RNA was extracted from the tissue using TRIzol® Reagent according to the manufacturer's instructions. RNA quality was assessed using a 5300 Bioanalyzer (Agilent) and quantified using an ND-2000 system (NanoDrop Technologies). The sequencing library was constructed only with only high-quality RNA samples ($OD_{260}/280 = 1.8-2.2$, $OD_{260}/230 \geq 2.0$, $RIN \geq 6.5$, $28S:18S \geq 1.0$, > 1 µg).

RNA purification, reverse transcription, library construction, and sequencing were performed at Shanghai Majorbio Biopharm Biotechnology Co., Ltd., following standard protocols specified by the manufacturer (Illumina, San Diego, CA). An RNA-seq transcriptome library was prepared using 1 µg of total RNA following the Illumina® Stranded mRNA Prep, Ligation Kit from Illumina (San Diego, CA). Briefly, messenger RNA was isolated using the polyA selection method with oligo (dT) beads. Then, the samples were fragmented using a fragmentation buffer. Next, double-stranded complementary DNA (cDNA) was synthesized using a SuperScript double-stranded cDNA synthesis kit (Invitrogen, CA) and random hexamer primers (Illumina). The synthesized cDNA was then subjected to end-repair, phosphorylation, and 'A' base addition following Illumina's library construction protocol. Libraries were selected based on the size of the cDNA target fragments of (300 bp) on a 2% low range ultra agarose. The products were subsequently amplified using Phusion DNA polymerase (NEB) with 15 polymerase chain reaction (PCR) cycles. After being quantified with a Qubit 4.0, the paired-end RNA-seq sequencing library was sequenced using a NovaSeq 6000 sequencer with a 2×150 bp read length.

The raw paired-end reads were trimmed and quality controlled by fastp, with default parameters. Then, the clean reads were separately aligned to the reference genome in orientation mode with HISAT2 software[7,8]. The mapped reads of each sample were assembled by StringTie *via* a reference-based approach to estimate the expression level of each gene in the sample[9]. Ultimately, StringTie combines the expression estimates of the individual transcripts and outputs the expression level of each gene, *i.e.*, the reads per million transcripts (TPM). The resulting TPM values were subsequently used for the subsequent differential gene expression analysis.

Differential expression analysis and functional enrichment

For identification of differentially expressed genes (DEGs) between different samples, the expression level of each transcript was calculated according to the TPM method. Transcript levels were determined using the TPM method. Gene abundances were quantified using RSEM[10]. Differential expression analysis was performed using the 'limma' package in the R software[11]. DEGs with a $|\log_2$ fold change > 1 and an adjusted *P*-value < 0.05 were considered significant DEGs. In addition, functional-enrichment analyses, including Gene Ontology (GO) and Kyoto Genome Encyclopedia (KEGG) analyses, were performed with the 'clusterProfiler' package in the R software[12], to identify which DEGs were significantly enriched in GO terms and metabolic pathways compared with the whole-transcriptome background. A Bonferroni-corrected *P*-value ≤ 0.05 was considered as the threshold for significant differences.

Immune cell infiltration

We used CIBERSORT, a deconvolution algorithm supported by the R package, to calculate the proportions of 22 immune cell types in each sample. The algorithm utilizes gene expression profiles to quantify immune infiltration and the reference signature matrix for CIBERSORT analysis is LM22[13]. First, we acquired the correspondence table for homologous genes of mice and humans from the Ensemble website (<https://asia.ensembl.org/index.html>). Then, we converted the mouse gene into a homologous human gene. We subsequently conducted a CIBERSORT analysis. Moreover, the results were validated by IHC.

Relative quantitative real-time PCR

The expression levels of key genes (S100a8 and Krt6b) were measured in the esophageal tissues of mice (NOR = 3, LGIN = 3, HGIN = 6, CA = 6). Total RNA was extracted from the esophageal samples using TRIzol reagent (Life Technologies, United States) according to the manufacturers' instructions. The synthesis of cDNA was conducted according to the RNA PCR kit protocol (TaKaRa Bio, China). Then, the cDNAs were subjected to PCR (for S100a8, Krt6b, and GAPDH) with SYBR Green reagents (Thermo Fisher Scientific, United States) under the reaction conditions. The primer sequences are shown in [Supplementary Table 1](#). The relative value of mRNA expression was calculated by the comparative $\Delta\Delta C_t$ method using GAPDH as a reference gene.

IHC

Protein expression in the esophageal tissues was assessed using immunohistochemical staining (NOR = 3, LGIN = 3, HGIN = 6, CA = 6). Following fixation with 10% formalin, the esophageal tissues were cut into 4 μm thick sections. The sections were dewaxed and rehydrated using xylene and ethanol. Endogenous peroxidase activity was inhibited by treating the sections with 3% H_2O_2 for 15 min. The sections were first blocked with 1% goat serum, and then antigen retrieval was performed by incubating the sections with Tris-EDTA buffer (pH = 9.0) for 10 min. Subsequently, the sections were washed three times for 3 min each and incubated with primary antibodies at 4 °C overnight. Thereafter, the samples were incubated with a biotinylated secondary antibody conjugated with streptavidin-biotinylated horseradish peroxidase.

Validation in mouse and human ESCC samples

First, we determined the mRNA and protein expression levels of key genes (S100a8 and Krt6b) in esophageal tissue samples from mice using relative quantitative real-time PCR (qPCR) and IHC, respectively. We then validated these results using formalin-fixed paraffin-embedded sections of esophageal precursor lesions collected from 31 patients at Cixian Cancer Hospital (Hebei Province, China) between 2021 and 2022; the sections were from the NOR ($n = 5$), LGIN ($n = 10$), HGIN ($n = 10$), and CA ($n = 6$) groups ([Supplementary Table 2](#)). The expression levels of S100a8 and Krt6b were determined through IHC staining of human specimens, and all the results were subjected to quantitative analysis using ImageJ. Approval for this study was obtained from the Institutional Ethics Committee of Cixian Cancer Hospital and China-Japan Friendship Hospital. Clinical information was retrieved from patients' medical records.

Cytokine assay

We determined the serum concentrations of interleukin (IL)-1 β , IL-2, IL-6, IL-10, IL-12, and tumor necrosis factor- α in mice using a Luminex multiplex cytokine kit following the instructions provided by the manufacturer.

Statistical analysis

All the statistical analyses were conducted with R software (version 4.1.0). Continuous data were analyzed by ANOVA (normally distributed data) or the Kruskal-Wallis test (non-normally distributed data). Categorical data were analyzed by the χ^2 methods. $P < 0.05$ was regarded as statistically significant.

RESULTS

Development of esophageal tumors

Here, we established a mouse model of EC using 4NQO ([Figure 1A](#)). In this study, 30 mice were treated with 4NQO while an additional five mice were not treated and served as the control group. By the end of the 24th wk, in the 4NQO-treated group, five mice had died, and the remaining 25 displayed varying degrees of malignant esophageal transformation. We observed a smooth surface and normal thickness in the NOR group, and the tissue did not show any unusual convexity or concavity. However, in the 4NQO group, the esophageal tissue exhibited thick, rough, white patches and palpable protuberances ([Supplementary Figure 1](#)). The esophageal epithelium in the 4NQO group exhibited LGIN ($n = 3$), HGIN ($n = 16$), and CA ($n = 6$, 1 CA *in situ*, 5 invasive CAs). HE staining revealed that the esophageal mucosal layer was thickened, the nuclei of the epithelial cells were enlarged and hyperchromatic, and the polarity of the cells disappeared in the LGIN and HGIN tissues. Furthermore, the esophageal mucosal layer was thickened in the LGIN and HGIN groups ([Figure 1B](#)). In addition, the expression levels of the malignant marker Ki-67 increased with the progression of esophageal pathology ([Figure 1C](#)). Pathology markers for SCC, specifically p40 ([Figure 1D](#)) and CK5 ([Figure 1E](#)), were found to be overexpressed in the LGIN, HGIN, and CA groups. These findings indicate that the induction of esophageal carcinogenesis by 4NQO in mice can replicate the pathological process implicated in the onset of ESCC in humans. Moreover, the tumor histology observed in this model predominantly revealed SCC.

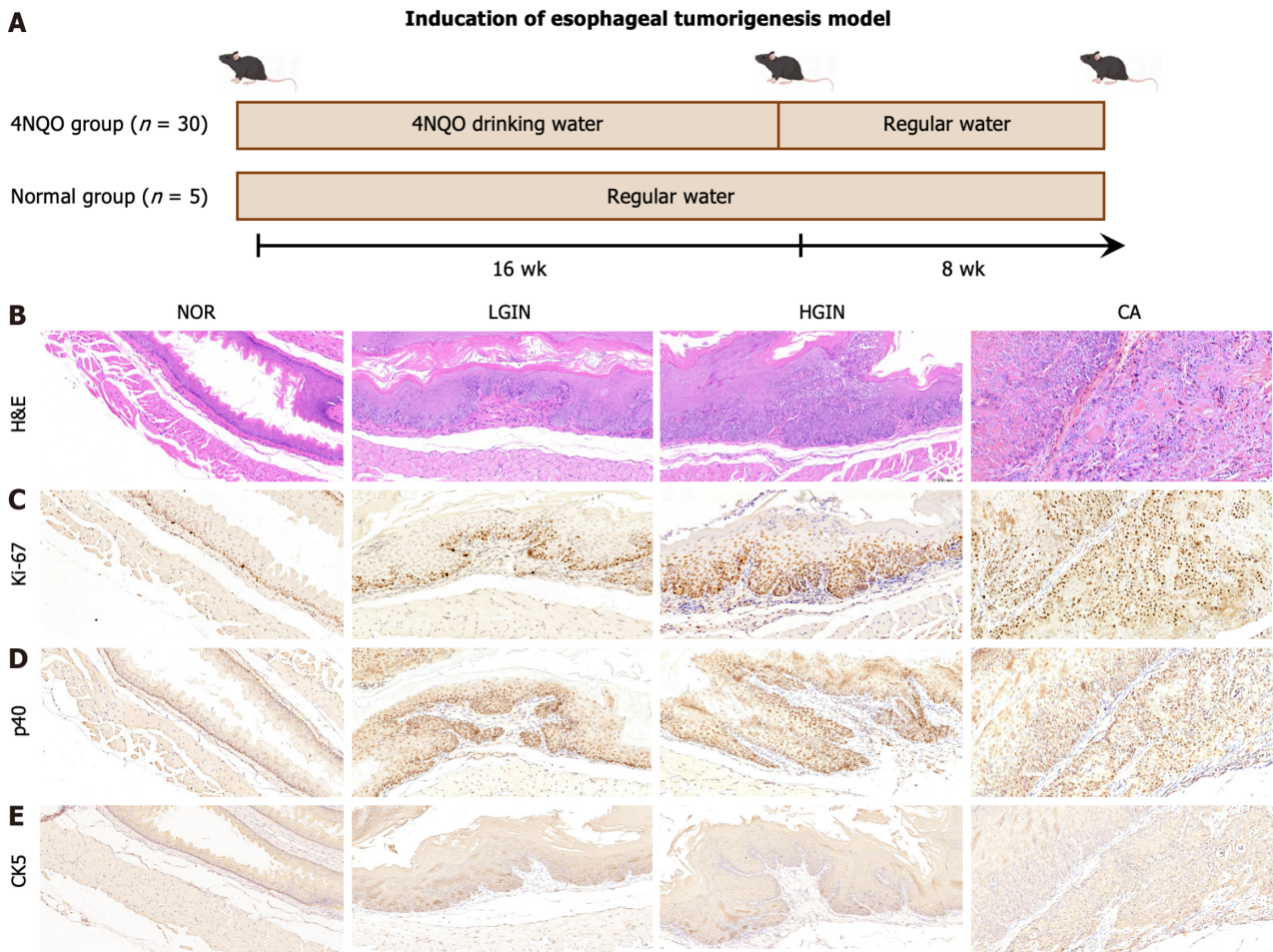


Figure 1 Development of esophageal tumor. A: The scheme of the induction for esophageal tumorigenesis model; B-E: Hematoxylin-eosin staining and expression of Ki67, p40, and CK5 were showed at multi-stage of esophageal squamous cell carcinoma development including normal, low-grade intraepithelial neoplasia, high-grade intraepithelial neoplasia, and carcinoma. 4NQO: 4-nitroquinoline 1-oxide; HE: Hematoxylin-eosin; LGIN: Low-grade intraepithelial neoplasia; HGIN: High-grade intraepithelial neoplasia; CA: Carcinoma; NOR: Normal.

Identifying DEGs during esophageal tumorigenesis

We performed a systemic differential expression analysis. Compared with those in the NOR group, 681 DEGs - 397 upregulated and 284 downregulated genes - were identified in the LGIN group. Similarly, 541 DEGs - 397 upregulated and 144 downregulated genes - were identified in the HGIN group and 840 DEGs - 634 upregulated and 206 downregulated genes - were found in the CA group (Figure 2A-C, Supplementary Tables 3-5).

Identification of key genes involved in the development of ESCC and functional enrichment analysis

The intersection between DEGs in the LGIN, HGIN, and CA groups was detected to identify the common key genes involved in the development of ESCC. In particular, to avoid confusion, we initially identified the upregulated DEGs in each group and performed an intersection analysis of these DEGs in the LGIN, HGIN, and CA groups. A total of 58 intersecting genes were identified (Figure 2D). We subsequently performed the same analysis for the downregulated DEGs and identified 28 intersecting genes (Figure 2E). Finally, 86 genes were identified that could be regarded as key genes in the development of ESCC (Supplementary Table 6). The most significant key genes, Krt6b, S100a8, Defb3, Sprr2h, Krt16, and Sprr2i, were annotated in the heatmap (Figure 2F).

Furthermore, these 86 genes were analyzed *via* GO and KEGG analyses to explore their functions. Among the biological process terms, 40 terms were enriched according to the GO enrichment analysis. These genes were enriched primarily in keratinization, keratinocyte differentiation, epidermal cell differentiation, and epidermis development (Figure 3A). Among the cellular component terms, 14 terms were enriched mainly in the cornified envelope, peptidase inhibitor, and apical part of the cell (Figure 3B). With respect to molecular function, which includes 26 terms, these genes were found to be enriched in structural constituents of the skin epidermis, endopeptidase activity, and peroxidase activity (Figure 3C). Here, we present only the 15 most enriched terms. The KEGG analysis revealed that these genes were predominantly involved in pathways such as IL-17 signaling, primary bile acid biosynthesis, and nitrogen metabolism (Figure 3D).

Infiltration of immune cells in the ESCC microenvironment

CIBERSORT software was used to estimate the abundance of immune cells in each sample[13]. Analysis of the abundance

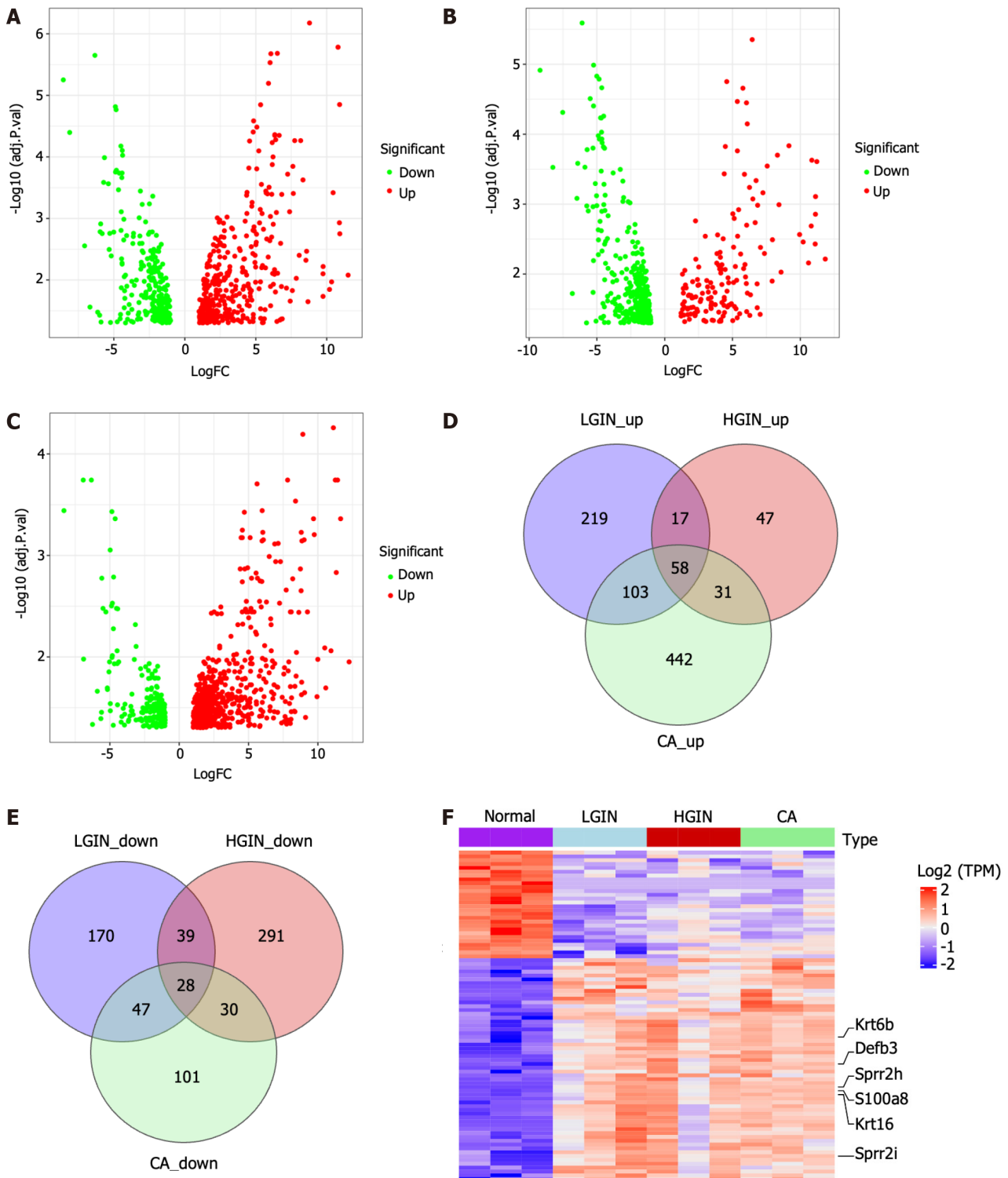


Figure 2 Differentially expressed gene analysis and identification of key genes in development of esophageal carcinogenesis. A-C: The volcano plots show the differentially expressed genes (DEGs) for low-grade intraepithelial neoplasia, high-grade intraepithelial neoplasia, and carcinoma (CA) compared to the normal, respectively; D and E: Venn diagrams of up-regulated and down-regulated DEGs; F: Heatmap of the 86 key genes. LGIN: Low-grade intraepithelial neoplasia; HGIN: High-grade intraepithelial neoplasia; CA: Carcinoma; NOR: Normal; TPM: Transcript per Kilobase per Million mapped reads.

of immune cells in the different groups revealed that compared to those in the normal group, M0 macrophages ($P < 0.05$) and M1 macrophages ($P < 0.05$) were more abundant in the 4NQO group (Figure 4A). The expression of M0 (CD68) and M1 (CD80 and CD86) markers was validated *via* immunohistochemical staining. The results showed that compared with the normal group, the 4NQO group with different pathological statuses (LGIN, HGIN, and CA) had a greater abundance of M0 and M1 macrophages than the normal group (Figure 4B-D).

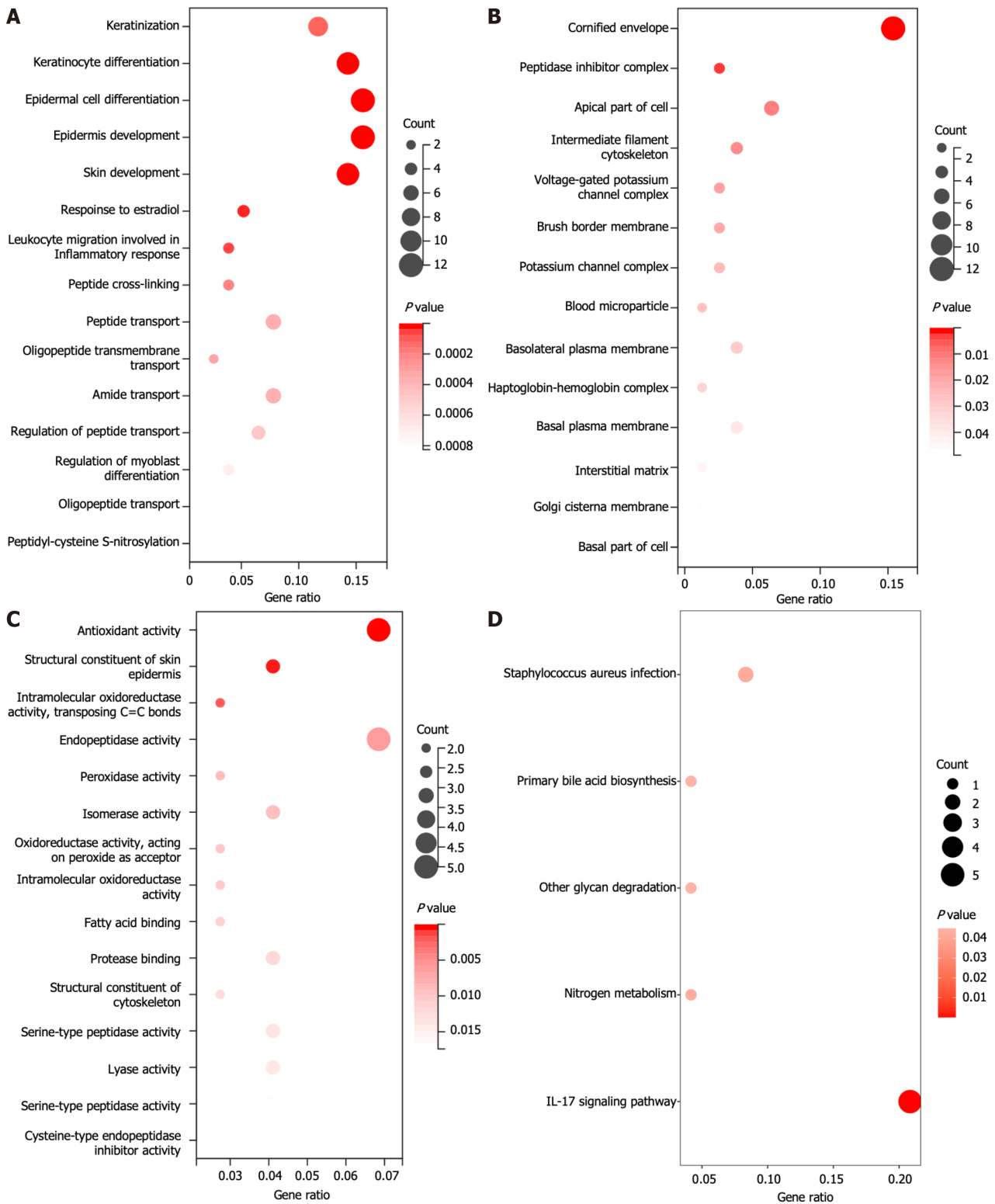


Figure 3 Functional enrichment analysis of key genes. A: Biological process terms; B: Cellular component terms; C: Molecular function terms; D: Kyoto Genome Encyclopedia signaling pathway terms. IL: Interleukin.

Expression of key genes in mouse and human samples

The top 2 key genes, *Krt6b* and *S100a8*, were selected for validation by qPCR and IHC. The qPCR results showed that both genes were highly expressed in the LGIN, HGIN, and CA groups compared with the NOR group (Figure 5A and B), consistent with the results of transcriptomic sequencing (Figure 5C and D). The protein levels of *S100a8* and *Krt6b* were overexpressed in the LGIN, HGIN, and CA groups as shown by the IHC results for mouse samples (Figure 6A and B). Furthermore, external human samples were utilized to confirm our findings in mice, and the IHC results indicated good consistency (Figure 6C and D). All the results were consistent, and the results are shown in Figure 6E-H.

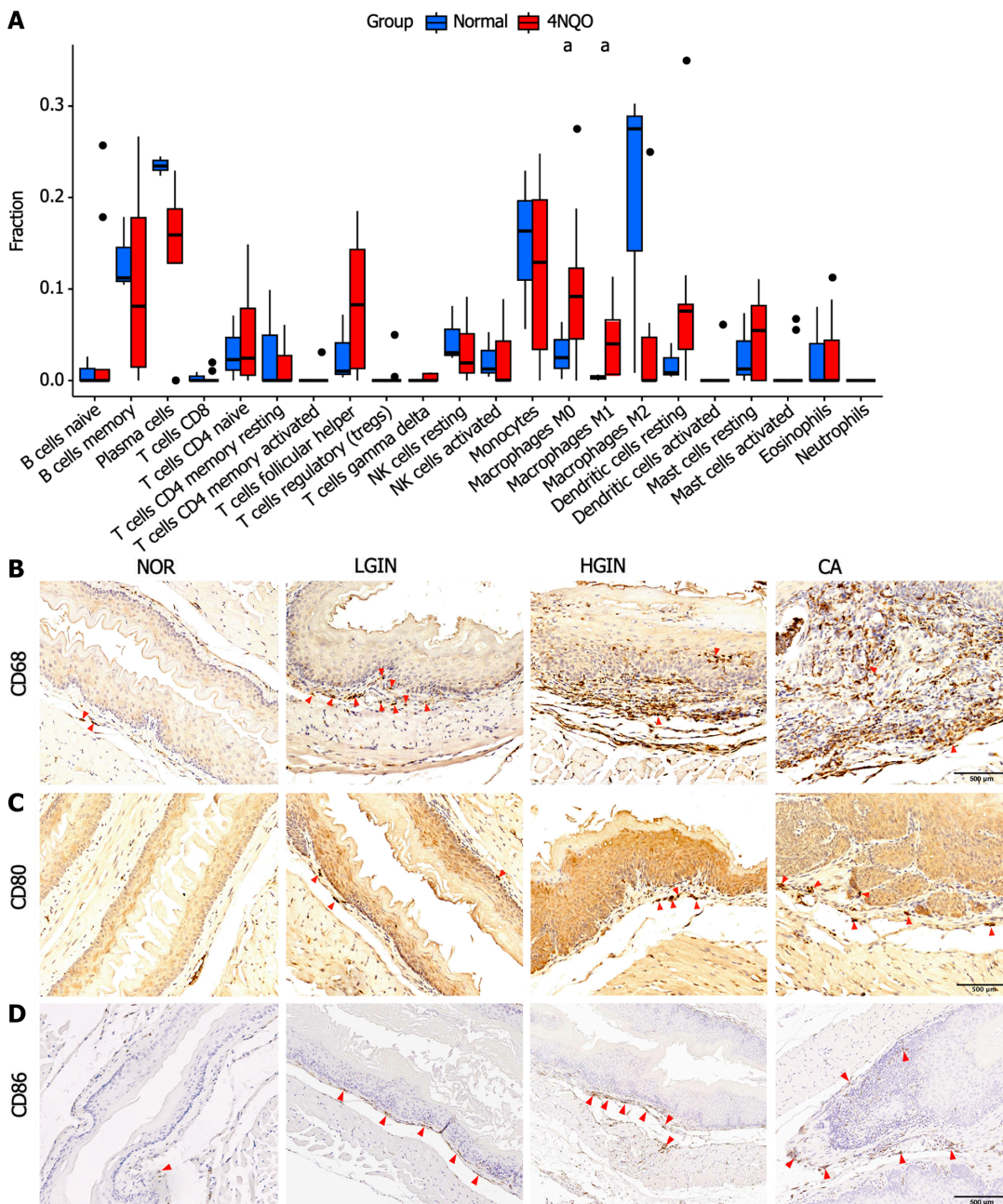


Figure 4 The immune infiltration pattern of the 4-nitroquinoline 1-oxide group compared to the normal group. A: Fraction of immune cell infiltration in 4-nitroquinoline 1-oxide (4NQO) carcinogenic intervention and normal (NOR) groups based on CIBERSORT algorithm; B-D: Expression of M0 (CD68) and M1 (CD80 and CD86) macrophage markers in NOR and 4NQO groups including low-grade intraepithelial neoplasia, high-grade intraepithelial neoplasia, and carcinoma. ^a $P < 0.05$. LGIN: Low-grade intraepithelial neoplasia; HGIN: High-grade intraepithelial neoplasia; CA: Carcinoma; NK: Natural killer.

The serum cytokine levels in mice

The serum cytokine analysis indicated that the serum levels of IL-1 β and IL-6 were increased and the serum levels of IL-10 were decreased in the LGIN, HGIN, and CA groups compared to the NOR group (Figure 7A-C). However, no significant differences in the expression of other cytokines were observed (Figure 7D-F).

DISCUSSION

ESCC is a multifactorial disease resulting from a complex interplay of genetic and environmental factors that leads to the gradual malignant transformation of esophageal epithelial cells. The progression of ESCC is a lengthy process, and precancerous lesions may persist for a prolonged period, making it difficult to obtain human samples representing different stages of carcinogenesis. To mimic the human ESCC, researchers have generated murine ESCC models *via* the exposure to 4NQO, a potent carcinogenic chemical[3]. The findings of our mouse model indicate its effectiveness in precisely pinpointing the genes implicated in the transition of normal epithelial cells to malignant epithelial cells.

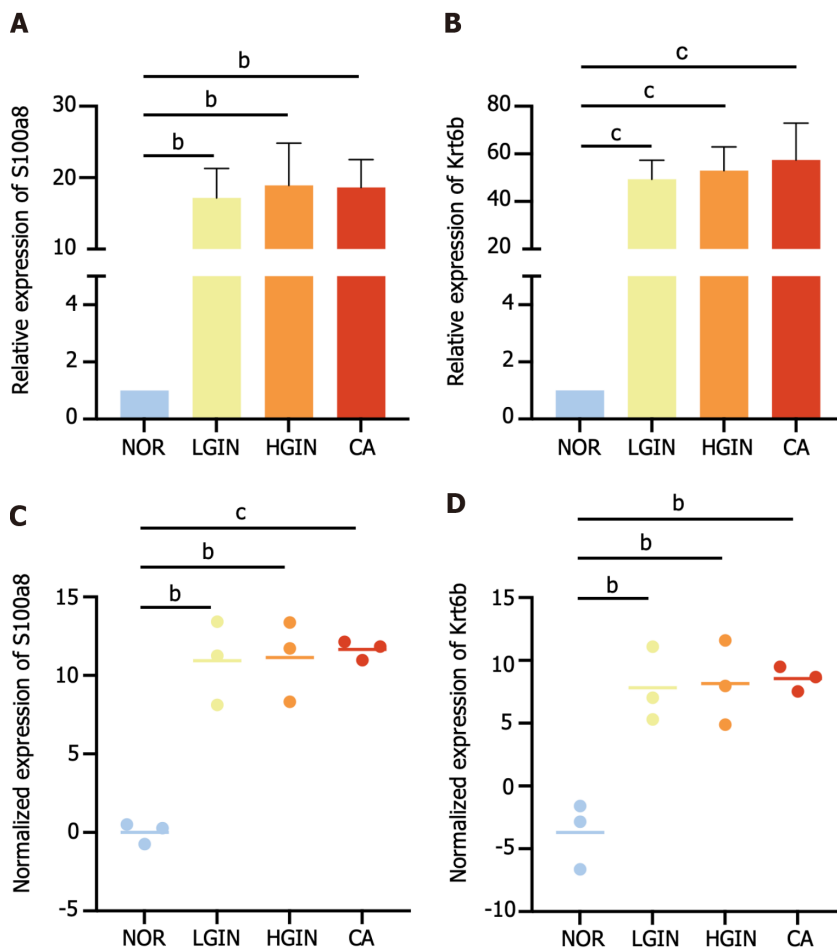


Figure 5 Expression of S100a8 and Krt6b at the transcriptional level. A and B: Expression of S100a8 and Krt6b were validated by relative quantitative real-time polymerase chain reaction; C and D: Expression of S100a8 and Krt6b in transcriptome sequencing. ^b $P < 0.01$, ^c $P < 0.001$. Low-grade intraepithelial neoplasia; HGIN: High-grade intraepithelial neoplasia; CA: Carcinoma; NOR: Normal.

In the present study, our results indicated that 4NQO can successfully induce atypical hyperplasia or cancerous changes in esophageal tissues at 24 wk. The multistage disease process in the murine model was similar to that in humans. The proliferative capacity of esophageal basal cells increases with disease progression, indicating a malignant transformation. Through transcriptome sequencing analysis, we identified 397 key genes that play crucial roles in the development of ESCC. Subsequently, functional enrichment analysis was performed to explore the biological function of these key genes. The results demonstrated that these genes were related to keratinization, keratinocyte differentiation, epidermal cell differentiation, and epithelial cell proliferation. Keratin constitutes the intermediate filament in epithelial cells. In cancer, keratin is extensively used as a diagnostic tumor marker, as epithelial malignancies largely express specific keratins associated with their origin. Several studies have shown that keratin may participate in cancer cell invasion and metastasis by regulating epithelial tumorigenesis[14]. The epidermis is formed and maintained by intricate genetic networks that link cellular differentiation processes, enzymatic activities, and cellular junctions. Disruption of these networks affects the balance between keratinocyte proliferation and differentiation, impairing epithelial integrity and leading to epidermal hyperproliferation and SCC. Recent studies on wound-induced and inflammation-mediated cancers in mice have identified the dysregulation of core barrier components as a major driver of tumor growth. Thus, it was hypothesized that the loss of barrier-related genes induces epithelial barrier dysfunction, inflammation-mediated epidermal hyperplasia, and carcinogenesis over time. This emerging perspective suggests that localized barrier impairment can be considered a hallmark of primary lesions in epidermal SCC under specific genetic circumstances[15].

Two representative key genes, namely Krt6b and S100a8, exhibited the most significant differences in expression and were validated by IHC. These genes are considered to play important roles in esophageal carcinogenesis. Krt6b, a member of the keratin gene family, can be detected in bladder cancer-derived exosomes and plays an important role in epithelial-mesenchymal transition and immune responses in bladder cancer[16]. Another study showed that Krt6b is upregulated in metastatic bladder tumors and that its expression in bladder cancer samples is positively correlated with tumor grade. In addition, Krt6b potentially functions as a marker for diagnosing and predicting the progression of melanoma[17]. S100a8 is a Ca^{2+} -binding protein that belongs to the S100 family. During inflammation, S100A8/A9 is actively released and modulates the inflammatory response by recruiting leukocytes and inducing cytokine secretion[18]. Numerous cancers originate from sites of infection, persistent irritation, and inflammation. The inflammatory microenvironment plays an essential role in the overproduction of inflammatory factors, thereby inducing neoplastic processes[19]. S100a8 also participates in several signaling pathways in tumor cells and contributes to tumor development, growth, and

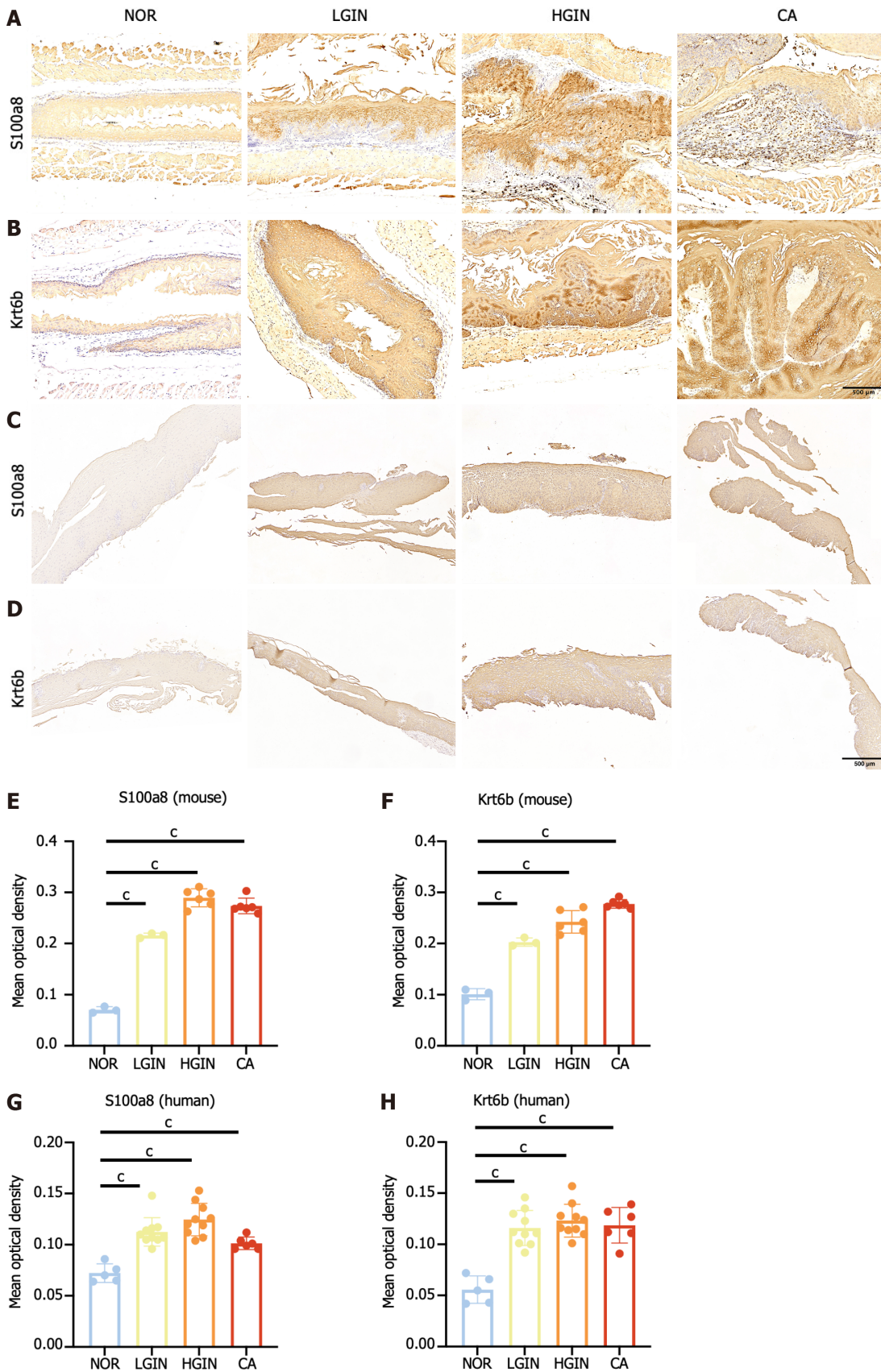


Figure 6 Validation of S100a8 and Krt6b. A and B: Protein expression of S100a8 and Krt6b in mouse; C and D: Validation of the protein expression of S100a8 and Krt6b in human samples; E-H: Quantitative analysis of immunohistochemical results of s100a8 and krt6b in mouse and human samples. $^{\circ}P < 0.001$. Low-grade intraepithelial neoplasia; HGIN: High-grade intraepithelial neoplasia; CA: Carcinoma; NOR: Normal.

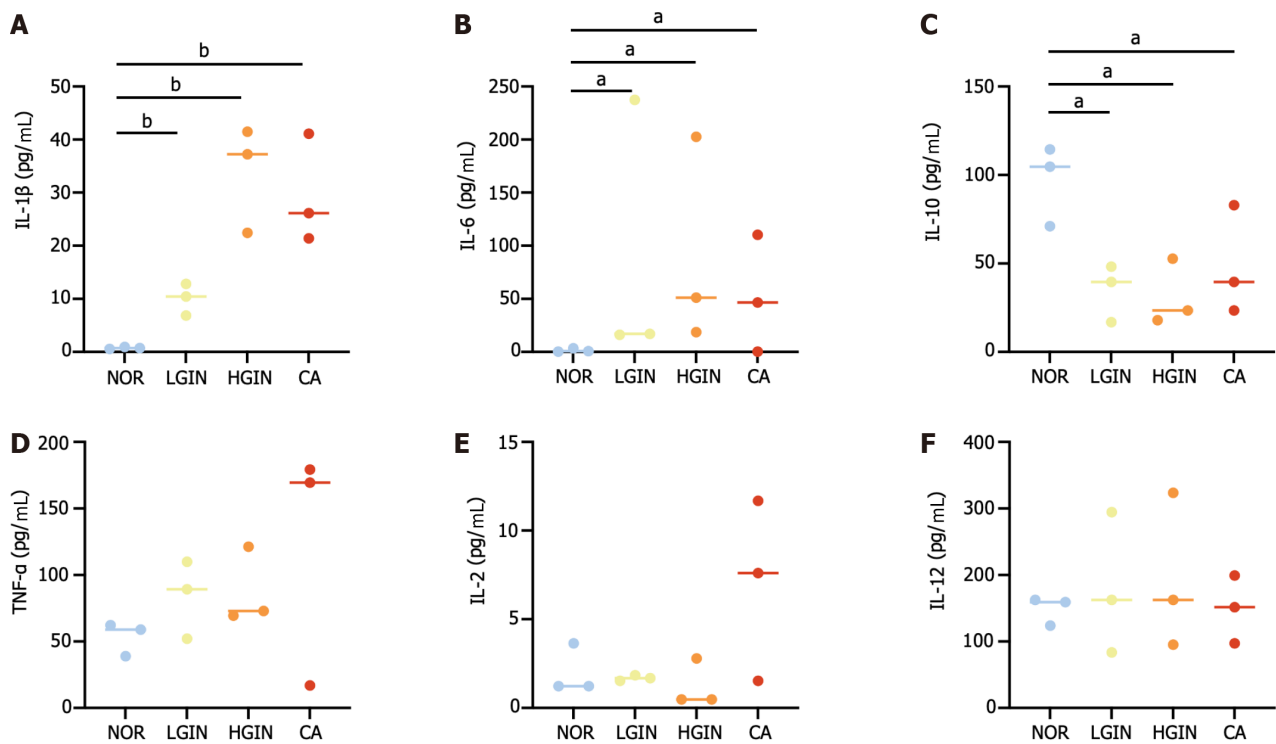


Figure 7 Expression of serum cytokines. A-F: Expression of inflammation-associated cytokines including interleukin (IL)-1 β , IL6, IL-10, tumor necrosis factor- α , IL-2, and IL-12. ^a $P < 0.05$, ^b $P < 0.01$. Low-grade intraepithelial neoplasia; HGIN: High-grade intraepithelial neoplasia; CA: Carcinoma; IL: Interleukin; TNF: Tumor necrosis factor.

metastasis by interfering with tumor metabolism and regulating the tumor microenvironment[20]. For instance, coculturing ESCC cells with macrophages enhances S100A8/9 expression and release by ESCC cells, promoting ESCC progression through the Akt and p38 MAPK signaling pathways[21]. S100A8 is highly expressed in colorectal cancer and promotes epithelial-mesenchymal transition and metastasis *via* the transforming growth factor- β /USF2 axis[22]. In addition, another study reported that by binding to NPTN β , S100A8/9 activates NFIA and NFIB to induce the invasion and metastasis of lung cancer cells[23].

In this study, CIBERSORT analysis revealed that, compared with the mice in the normal group, the mice in the 4NQO group had a high abundance of M0 and M1 macrophages in their esophagus. Chronic inflammation plays an important role in the initiation and development of various cancers, particularly in digestive organs[24]. Macrophages, as crucial components of innate immunity, are closely related to inflammatory and immune responses. During tumor initiation, macrophages form an inflammatory microenvironment that promotes mutation and growth. As tumors progress to malignancy, macrophages stimulate angiogenesis, enhance tumor cell migration and invasion, and suppress antitumor immunity[25]. Numerous clinical and experimental studies have shown that macrophages promote cancer initiation and malignant progression. For example, in one meta-analysis, more than 80% of studies reported a correlation between macrophage abundance and poor patient prognosis of patients[26-28]. In ESCA, another study showed that after a surgical model of gastroesophageal reflux disease was established, numerous CD68+ macrophages surrounding squamous proliferative hyperplasia, Barrett's metaplasia (BM), AC, and SCC were identified, while moderate infiltration of CD163+ macrophages was observed in BM, AC, and SCC[29]. These findings demonstrate the accretive effect of macrophages on esophageal carcinogenesis. Thus, macrophage infiltration induced by chronic inflammation may be involved in esophageal carcinogenesis.

Additionally, the study showed that inflammatory cytokines including IL-1 β , IL-6, and IL-10 were dysregulated in peripheral blood. Previous studies have shown that transgenic mice that overexpress IL-1 β in the esophagus can develop squamous epithelial atypia and subsequently develop SCC over time[30]. Another study suggested that the overexpression of IL-1 β was related to poor prognosis in patients with SCC and may be a promising molecular target for SCC therapeutic intervention[31]. IL-6 has been well studied in SCC; for instance, positive IL-6 staining was linked to the development of distant metastasis and decreased treatment response rates. In addition, the serum IL-6 concentration was significantly elevated in patients who developed disease failure. When IL-6 expression is inhibited, aggressive tumor behavior and radiation resistance can be overcome *in vitro* and *in vivo*[32]. Another study revealed that polymorphism in IL-10 were more common found in patients with Barrett's disease or AC and were previously reported to be associated with chronic inflammation[33,34]. In summary, these results suggest that an imbalance in inflammation regulation could contribute to the development of ESCC.

The concept of multistage development of ESCC has been described previously. The strength of the present study is that we identified a group of genes that are possibly involved in esophageal tumorigenesis through transcriptome sequencing and bioinformatic analysis. Furthermore, the irregular infiltration of macrophages indicates chronic inflammation in the microenvironment of the esophagus, which may drive the process of carcinogenesis. Moreover, dysregu-

lation of inflammation-related cytokines in the blood periphery implies a close correlation between inflammation and EC. Despite these strengths, our study inevitably has several limitations as well. First, because there is a lack of sequencing data focused on esophageal carcinogenesis, an ideal external dataset was not been found to validate the results of this study. Second, further functional experiments are required to investigate the biomarkers identified through transcriptome sequencing. In summary, subsequent validation in a clinical dataset and the use of additional experiments to validate the molecular function of the biomarkers will be the focus of our future research.

CONCLUSION

We induced esophageal carcinogenesis with 4NQO. HE staining confirmed the involvement of a multistage process in the development of ESCC. Then, we performed RNA-seq and utilized bioinformatics to identify key genes involved in the development of ESCC. The results revealed a group of key genes, and the functional enrichment analysis revealed that these genes were associated with keratinization, epidermal cell differentiation, epidermal development, and epithelial cell proliferation. KEGG pathway analysis revealed inflammation-related and cancer-related signals, such as those related to IL-17. Cytokine-cytokine receptor interactions and transcriptional dysregulation may be involved in the development of EC. The CIBERSORT analysis revealed differences in the abundances of M0 and M1 macrophages between the 4NQO and normal groups. Furthermore, *via* IHC, we validated the results of transcriptome sequencing by measuring the expression of the two key genes (S100a8 and Krt6b) and macrophage markers.

ARTICLE HIGHLIGHTS

Research background

Precancerous lesions including low-grade intraepithelial neoplasia (LGIN) and high-grade IN (HGIN) are a mandatory stage in the development of esophageal squamous cell carcinoma (ESCC). The regulatory molecules driving esophageal carcinogenesis remain unclear, which largely hampers early esophageal cancer diagnosis and treatment.

Research motivation

We aimed to establish a mouse model mimicking the multi-stage development of ESCC and then to examine the key genes involved in the development of ESCC through transcriptome sequencing. Besides, we aimed to explore the immune cell infiltration in the microenvironment associated with the multi-stage progression of ESCC. Additionally, we hope to validate our results using human samples, which may provide a novel perspective for clinical application.

Research objectives

To examine the genes and immune cell infiltration in the microenvironment associated with the multi-stage progression of ESCC to facilitate diagnosis and early intervention.

Research methods

The mouse model of esophageal tumorigenesis was established by providing 4-nitroquinoline 1-oxide (4NQO) containing water to C57BL/6 mice. The transcriptome sequencing was performed for esophageal tissues with different pathological statuses. Differentially expressed gene analysis (DEGA) and Venn diagram were used to identify key genes. Gene Ontology (GO) and Kyoto Encyclopedia of Genes and Genomes (KEGG) enrichment analysis were used to explore the biological function of genes. The CIBERSORT algorithm was used to detect the pattern of immune cell infiltration. The immunohistochemistry (IHC) was conducted to validate our results. Furthermore, the Luminex multiplex cytokines analysis was utilized to measure the serum level of cytokines in mice.

Research results

A total of 86 genes were identified as key genes in the development of ESCC. Enrichment analysis showed that these genes were mainly enriched in keratinization, epidermal cell differentiation, and interleukin (IL)-17 signaling pathways. CIBERSORT analysis showed that the esophageal carcinogenesis group had more infiltration of M0 and M1 macrophages which was then validated by IHC. Serum cytokines analysis showed that IL-1 β and IL-6 were upregulated, while IL-10 was downregulated in LGIN, HGIN, and carcinoma groups. Moreover, the expression of the representative key genes, like S100a8 and Krt6b, was verified in external human samples, and the results of immunohistochemical staining were consistent with the findings in mice.

Research conclusions

We identified a set of key genes represented by S100a8 and Krt6b and investigated their potential biological functions. In addition, we found that macrophage infiltration and abnormal alterations of inflammation-associated cytokines, such as IL-1 β , IL-6, and IL-10, in the peripheral blood may be closely associated with the development of ESCC.

Research perspectives

We have identified a set of key genes that are closely associated with esophageal carcinogenesis and may serve as novel

biomarkers for early detection of ESCC. Additionally, the aberrant infiltration of inflammatory macrophages and dysregulation of cytokines may contribute to esophageal carcinogenesis.

ACKNOWLEDGEMENTS

We thank the editors for their kind work and the reviewers for their constructive comments.

FOOTNOTES

Author contributions: Sun JR and Jia LQ designed the study and modified the manuscript; Sun JR and Chen DM carried out the data extraction and statistical analysis; Sun JR, Chen DM, Huang R, and Wang RT drafted the manuscript; and all authors contributed to the article and approved the submitted version.

Supported by National Natural Foundation of China, No. 82174223; and 2019 Chinese and Western Medicine Clinical Collaborative Capacity Building Project for Major Difficult Diseases, No. 2019-ZX-005.

Institutional review board statement: The research involving human tissue samples was approved by the Institutional Ethics Committee of Cixian Cancer Hospital (2019-CXCH-19) and China-Japan Friendship Hospital (2019-190-K131).

Institutional animal care and use committee statement: All the animal procedures and experiments conducted in the current study were approved by the Animal Ethics Committee of the China-Japan Friendship Hospital (Permit No. ZRDWLL20230210).

Conflict-of-interest statement: All the authors report no relevant conflicts of interest for this article.

Data sharing statement: The data used to support the findings of this study are available from the corresponding author upon request.

ARRIVE guidelines statement: The authors have read the ARRIVE guidelines, and the manuscript was prepared and revised according to the ARRIVE guidelines.

Open-Access: This article is an open-access article that was selected by an in-house editor and fully peer-reviewed by external reviewers. It is distributed in accordance with the Creative Commons Attribution NonCommercial (CC BY-NC 4.0) license, which permits others to distribute, remix, adapt, build upon this work non-commercially, and license their derivative works on different terms, provided the original work is properly cited and the use is non-commercial. See: <https://creativecommons.org/licenses/by-nc/4.0/>

Country/Territory of origin: China

ORCID number: Li-Qun Jia [0009-0002-3513-5768](https://orcid.org/0009-0002-3513-5768).

S-Editor: Wang JJ

L-Editor: A

P-Editor: Zhang XD

REFERENCES

- 1 **Sung H**, Ferlay J, Siegel RL, Laversanne M, Soerjomataram I, Jemal A, Bray F. Global Cancer Statistics 2020: GLOBOCAN Estimates of Incidence and Mortality Worldwide for 36 Cancers in 185 Countries. *CA Cancer J Clin* 2021; **71**: 209-249 [PMID: [33538338](https://pubmed.ncbi.nlm.nih.gov/33538338/) DOI: [10.3322/caac.21660](https://doi.org/10.3322/caac.21660)]
- 2 **Morgan E**, Soerjomataram I, Rungay H, Coleman HG, Thrift AP, Vignat J, Laversanne M, Ferlay J, Arnold M. The Global Landscape of Esophageal Squamous Cell Carcinoma and Esophageal Adenocarcinoma Incidence and Mortality in 2020 and Projections to 2040: New Estimates From GLOBOCAN 2020. *Gastroenterology* 2022; **163**: 649-658.e2 [PMID: [35671803](https://pubmed.ncbi.nlm.nih.gov/35671803/) DOI: [10.1053/j.gastro.2022.05.054](https://doi.org/10.1053/j.gastro.2022.05.054)]
- 3 **Tang XH**, Knudsen B, Bemis D, Tickoo S, Gudas LJ. Oral cavity and esophageal carcinogenesis modeled in carcinogen-treated mice. *Clin Cancer Res* 2004; **10**: 301-313 [PMID: [14734483](https://pubmed.ncbi.nlm.nih.gov/14734483/) DOI: [10.1158/1078-0432.CCR-0999-3](https://doi.org/10.1158/1078-0432.CCR-0999-3)]
- 4 **Chu J**, Niu X, Chang J, Shao M, Peng L, Xi Y, Lin A, Wang C, Cui Q, Luo Y, Fan W, Chen Y, Sun Y, Guo W, Tan W, Lin D, Wu C. Metabolic remodeling by TIGAR overexpression is a therapeutic target in esophageal squamous-cell carcinoma. *Theranostics* 2020; **10**: 3488-3502 [PMID: [32206103](https://pubmed.ncbi.nlm.nih.gov/32206103/) DOI: [10.7150/thno.41427](https://doi.org/10.7150/thno.41427)]
- 5 **Dawsey SM**, Lewin KJ, Wang GQ, Liu FS, Nieberg RK, Yu Y, Li JY, Blot WJ, Li B, Taylor PR. Squamous esophageal histology and subsequent risk of squamous cell carcinoma of the esophagus. A prospective follow-up study from Linxian, China. *Cancer* 1994; **74**: 1686-1692 [PMID: [8082069](https://pubmed.ncbi.nlm.nih.gov/8082069/) DOI: [10.1002/1097-0142\(19940915\)74:6<1686::aid-cnrcr2820740608>3.0.co;2-v](https://doi.org/10.1002/1097-0142(19940915)74:6<1686::aid-cnrcr2820740608>3.0.co;2-v)]
- 6 **Yao J**, Cui Q, Fan W, Ma Y, Chen Y, Liu T, Zhang X, Xi Y, Wang C, Peng L, Luo Y, Lin A, Guo W, Lin L, Lin Y, Tan W, Lin D, Wu C, Wang J. Single-cell transcriptomic analysis in a mouse model deciphers cell transition states in the multistep development of esophageal cancer. *Nat Commun* 2020; **11**: 3715 [PMID: [32709844](https://pubmed.ncbi.nlm.nih.gov/32709844/) DOI: [10.1038/s41467-020-17492-y](https://doi.org/10.1038/s41467-020-17492-y)]
- 7 **Chen S**, Zhou Y, Chen Y, Gu J. fastp: an ultra-fast all-in-one FASTQ preprocessor. *Bioinformatics* 2018; **34**: i884-i890 [PMID: [30423086](https://pubmed.ncbi.nlm.nih.gov/30423086/) DOI: [10.1093/bioinformatics/bty560](https://doi.org/10.1093/bioinformatics/bty560)]

- 8 **Kim D**, Langmead B, Salzberg SL. HISAT: a fast spliced aligner with low memory requirements. *Nat Methods* 2015; **12**: 357-360 [PMID: 25751142 DOI: 10.1038/nmeth.3317]
- 9 **Pertea M**, Pertea GM, Antonescu CM, Chang TC, Mendell JT, Salzberg SL. StringTie enables improved reconstruction of a transcriptome from RNA-seq reads. *Nat Biotechnol* 2015; **33**: 290-295 [PMID: 25690850 DOI: 10.1038/nbt.3122]
- 10 **Li B**, Dewey CN. RSEM: accurate transcript quantification from RNA-Seq data with or without a reference genome. *BMC Bioinformatics* 2011; **12**: 323 [PMID: 21816040 DOI: 10.1186/1471-2105-12-323]
- 11 **Ritchie ME**, Phipson B, Wu D, Hu Y, Law CW, Shi W, Smyth GK. limma powers differential expression analyses for RNA-sequencing and microarray studies. *Nucleic Acids Res* 2015; **43**: e47 [PMID: 25605792 DOI: 10.1093/nar/gkv007]
- 12 **Yu G**, Wang LG, Han Y, He QY. clusterProfiler: an R package for comparing biological themes among gene clusters. *OMICS* 2012; **16**: 284-287 [PMID: 22455463 DOI: 10.1089/omi.2011.0118]
- 13 **Newman AM**, Liu CL, Green MR, Gentles AJ, Feng W, Xu Y, Hoang CD, Diehn M, Alizadeh AA. Robust enumeration of cell subsets from tissue expression profiles. *Nat Methods* 2015; **12**: 453-457 [PMID: 25822800 DOI: 10.1038/nmeth.3337]
- 14 **Karantza V**. Keratins in health and cancer: more than mere epithelial cell markers. *Oncogene* 2011; **30**: 127-138 [PMID: 20890307 DOI: 10.1038/onc.2010.456]
- 15 **Darido C**, Georgy SR, Jane SM. The role of barrier genes in epidermal malignancy. *Oncogene* 2016; **35**: 5705-5712 [PMID: 27041586 DOI: 10.1038/onc.2016.84]
- 16 **Song Q**, Yu H, Cheng Y, Han J, Li K, Zhuang J, Lv Q, Yang X, Yang H. Bladder cancer-derived exosomal KRT6B promotes invasion and metastasis by inducing EMT and regulating the immune microenvironment. *J Transl Med* 2022; **20**: 308 [PMID: 35794606 DOI: 10.1186/s12967-022-03508-2]
- 17 **Liu YR**, Yin PN, Silvers CR, Lee YF. Enhanced metastatic potential in the MB49 urothelial carcinoma model. *Sci Rep* 2019; **9**: 7425 [PMID: 31092844 DOI: 10.1038/s41598-019-43641-5]
- 18 **Wang S**, Song R, Wang Z, Jing Z, Wang S, Ma J. S100A8/A9 in Inflammation. *Front Immunol* 2018; **9**: 1298 [PMID: 29942307 DOI: 10.3389/fimmu.2018.01298]
- 19 **Shabani F**, Farasat A, Mahdavi M, Gheibi N. Calprotectin (S100A8/S100A9): a key protein between inflammation and cancer. *Inflamm Res* 2018; **67**: 801-812 [PMID: 30083975 DOI: 10.1007/s00011-018-1173-4]
- 20 **Chen Y**, Ouyang Y, Li Z, Wang X, Ma J. S100A8 and S100A9 in Cancer. *Biochim Biophys Acta Rev Cancer* 2023; **1878**: 188891 [PMID: 37001615 DOI: 10.1016/j.bbcan.2023.188891]
- 21 **Tanigawa K**, Tsukamoto S, Koma YI, Kitamura Y, Urakami S, Shimizu M, Fujikawa M, Kodama T, Nishio M, Shigeoka M, Kakeji Y, Yokozaki H. S100A8/A9 Induced by Interaction with Macrophages in Esophageal Squamous Cell Carcinoma Promotes the Migration and Invasion of Cancer Cells via Akt and p38 MAPK Pathways. *Am J Pathol* 2022; **192**: 536-552 [PMID: 34954212 DOI: 10.1016/j.ajpath.2021.12.002]
- 22 **Li S**, Zhang J, Qian S, Wu X, Sun L, Ling T, Jin Y, Li W, Lai M, Xu F. S100A8 promotes epithelial-mesenchymal transition and metastasis under TGF- β /USF2 axis in colorectal cancer. *Cancer Commun (Lond)* 2021; **41**: 154-170 [PMID: 33389821 DOI: 10.1002/cac2.12130]
- 23 **Sumardika IW**, Chen Y, Tomonobu N, Kinoshita R, Ruma IMW, Sato H, Kondo E, Inoue Y, Yamauchi A, Murata H, Yamamoto KI, Tomida S, Shien K, Yamamoto H, Soh J, Futami J, Putranto EW, Hibino T, Nishibori M, Toyooka S, Sakaguchi M. Neuroplastin- β mediates S100A8/A9-induced lung cancer disseminative progression. *Mol Carcinog* 2019; **58**: 980-995 [PMID: 30720226 DOI: 10.1002/mc.22987]
- 24 **Chiba T**, Marusawa H, Ushijima T. Inflammation-associated cancer development in digestive organs: mechanisms and roles for genetic and epigenetic modulation. *Gastroenterology* 2012; **143**: 550-563 [PMID: 22796521 DOI: 10.1053/j.gastro.2012.07.009]
- 25 **Qian BZ**, Pollard JW. Macrophage diversity enhances tumor progression and metastasis. *Cell* 2010; **141**: 39-51 [PMID: 20371344 DOI: 10.1016/j.cell.2010.03.014]
- 26 **Bingle L**, Brown NJ, Lewis CE. The role of tumour-associated macrophages in tumour progression: implications for new anticancer therapies. *J Pathol* 2002; **196**: 254-265 [PMID: 11857487 DOI: 10.1002/path.1027]
- 27 **Feng Q**, Chang W, Mao Y, He G, Zheng P, Tang W, Wei Y, Ren L, Zhu D, Ji M, Tu Y, Qin X, Xu J. Tumor-associated Macrophages as Prognostic and Predictive Biomarkers for Postoperative Adjuvant Chemotherapy in Patients with Stage II Colon Cancer. *Clin Cancer Res* 2019; **25**: 3896-3907 [PMID: 30988081 DOI: 10.1158/1078-0432.CCR-18-2076]
- 28 **Troiano G**, Caponio VCA, Adipietro I, Tepedino M, Santoro R, Laino L, Lo Russo L, Cirillo N, Lo Muzio L. Prognostic significance of CD68(+) and CD163(+) tumor associated macrophages in head and neck squamous cell carcinoma: A systematic review and meta-analysis. *Oral Oncol* 2019; **93**: 66-75 [PMID: 31109698 DOI: 10.1016/j.oraloncology.2019.04.019]
- 29 **Miyashita T**, Tajima H, Shah FA, Oshima M, Makino I, Nakagawara H, Kitagawa H, Fujimura T, Harmon JW, Ohta T. Impact of inflammation-metaplasia-adenocarcinoma sequence and inflammatory microenvironment in esophageal carcinogenesis using surgical rat models. *Ann Surg Oncol* 2014; **21**: 2012-2019 [PMID: 24526548 DOI: 10.1245/s10434-014-3537-5]
- 30 **Muthupalani S**, Annamalai D, Feng Y, Ganesan SM, Ge Z, Whary MT, Nakagawa H, Rustgi AK, Wang TC, Fox JG. IL-1 β transgenic mouse model of inflammation driven esophageal and oral squamous cell carcinoma. *Sci Rep* 2023; **13**: 12732 [PMID: 37543673 DOI: 10.1038/s41598-023-39907-8]
- 31 **Chen MF**, Lu MS, Chen PT, Chen WC, Lin PY, Lee KD. Role of interleukin 1 beta in esophageal squamous cell carcinoma. *J Mol Med (Berl)* 2012; **90**: 89-100 [PMID: 21912958 DOI: 10.1007/s00109-011-0809-4]
- 32 **Chen MF**, Chen PT, Lu MS, Lin PY, Chen WC, Lee KD. IL-6 expression predicts treatment response and outcome in squamous cell carcinoma of the esophagus. *Mol Cancer* 2013; **12**: 26 [PMID: 23561329 DOI: 10.1186/1476-4598-12-26]
- 33 **Gough MD**, Ackroyd R, Majeed AW, Bird NC. Prediction of malignant potential in reflux disease: are cytokine polymorphisms important? *Am J Gastroenterol* 2005; **100**: 1012-1018 [PMID: 15842572 DOI: 10.1111/j.1572-0241.2005.40904.x]
- 34 **Liu X**, Zhang M, Ying S, Zhang C, Lin R, Zheng J, Zhang G, Tian D, Guo Y, Du C, Chen Y, Chen S, Su X, Ji J, Deng W, Li X, Qiu S, Yan R, Xu Z, Wang Y, Cui J, Zhuang S, Yu H, Zheng Q, Marom M, Sheng S, Hu S, Li R, Su M. Genetic Alterations in Esophageal Tissues From Squamous Dysplasia to Carcinoma. *Gastroenterology* 2017; **153**: 166-177 [PMID: 28365443 DOI: 10.1053/j.gastro.2017.03.033]



Published by **Baishideng Publishing Group Inc**
7041 Koll Center Parkway, Suite 160, Pleasanton, CA 94566, USA
Telephone: +1-925-3991568
E-mail: office@baishideng.com
Help Desk: <https://www.f6publishing.com/helpdesk>
<https://www.wjgnet.com>

